BULLETIN OF THE POLISH ACADEMY OF SCIENCES
TECHNICAL SCIENCES, Vol. 59, No. 4, 2011
DOI: 10.2478/v10175-011-0061-7

Review and comparison of high efficiency high power boost DC/DC converters for photovoltaic applications

J. DAWIDZIUK*

Faculty of Electrical Engineering, Department of Automatic Control Engineering and Electronics, Bialystok University of Technology, 45D Wiejska St. 15-351 Bialystok, Poland

Abstract. Recent environmental issues have accelerated the use of more efficient and energy saving technologies in renewable energy systems. High power high efficiency boost DC/DC converters for the use in photovoltaic, fuel cell systems are discussed in this paper from the viewpoint of power losses and efficiency. State of the art converters with switching frequency within the range of 25 kHz with IGBTs to 100 kHz with power MOSFETs and the highest efficiency close to 98%, depending on the load conditions, is considered. A comparison and discussion of the highest efficiency high power DC/DC boost converters is also presented in this paper.

Key words: boost DC/DC converters, high efficiency, high power, photovoltaic systems, renewable energy.

1. Introduction

In many renewable energy applications high efficiency, high power, high voltage boost DC/DC converters are required as an integral interface between the available low voltage sources and the output loads, which operate at higher voltages. Examples are energy storage components such as batteries, and ultracapacitors which are used in the power trains of hybrid electric vehicles, electric vehicles, and fuel cell vehicles. In the modern power drive, the voltage levels of the energy storage devices are predominantly low when the motors of the vehicles are driven at much higher voltages. In the computer industry and in the telecommunication batteries with low voltage levels are utilized as a back-up power source .

Another example is automotive headlamps which use high-intensity discharge lamp ballasts. The DC/DC converter is required to boost the low voltage of the car battery to much higher voltage during start-up and normal operation. Examples of recent applications are photovoltaic cells that require high-gain dc voltage conversion. In all of these applications, non-isolated boost DC/DC converters can be used but they should operate at high efficiency while conducting high currents from low-voltage dc sources at their inputs.

The duty cycle of a conventional boost converter increases with the increase of the voltage gain. For applications requiring high voltage gain (8 or higher) it becomes a problem to maintain high efficiency because of the high duty cycle. In practical applications it causes additional voltage stresses and necessitates the use of switches with a high blocking voltage rating, thus introducing more losses.

Low input voltage results in large currents flowing through the switches. While working at maximum duty cycle current spikes of high amplitude flow through output capacitors and output diodes causing serious problems with diode reverse recovery. They also increase switching and conduction losses. High R_{on} resistance of the switches increases conduction losses and the reverse recovery problem can reduce efficiency. Moreover the parasitic components introduce additional voltage overshoots creating the necessity to use switches with higher blocking voltages, which further increases losses.

The demand for power converters working with low voltage sources has increased in the last decade, especially in the area of renewable energy sources, including photovoltaic systems.

2. Structures of a photovoltaic system

The main parts of a photovoltaic system (PV) are: photovoltaic panels (also called photovoltaic cells), DC/DC and/or DC/AC converters, energy storage and control systems and control-measuring devices.

DC/DC and DC/AC converters are a main part of a network-connected photovoltaic system. The main task for the converter is to increase the inverter DC voltage and convert the DC to AC domain.

A single PV cell without load produces output voltage up to 0.6 V. To increase the output voltage and output current single cells are connected in series and in parallel to form PV panels. Most of commercial PV panels deliver power in the range of 100 to 400 Watts at output voltage of 20 to 45 V (from a single panel). To increase output power the panels are grouped in strings and arrays.

Grid connected PV inverters can be divided into four main structures: central inverters, string inverters, PV module integrated or module-oriented inverters and multi-string inverters.

PV panels can be isolated or have no galvanic isolation from the power grid. Galvanic isolation is usually implemented by means of a transformer which affects overall efficiency of the photovoltaic systems. In some countries there is an obligation to use electrical isolation. Lack of isolation between

*e-mail: dawid@pb.edu.pl

the input and the output in a non-isolated power conversion systems creates problems with the ground input power source. The disadvantage of converters with transformer isolation is the possibility of transformer core saturation, which leads to a decrease of the system's efficiency.

Statistical research carried out on more than 400 converters in the power range from a few hundred watts to 6.5 kW, proves that transformerless systems demonstrate the highest efficiency at 93 to 98%, the lowest weight at 4.5 kg/kW, and the smallest volume at 6 dcm^3/kW. Isolated converters with low and high frequency transformers were characterized by 92 to 96% efficiency, weight of 5 to 12 kg/kW and volume of 10 to 12 dcm^3/kW [1].

Converters with high frequency transformers have been commonly used for many years. However, when there is no necessity to use galvanic isolation between the input and the output, use of non-isolated boost DC/DC converters is the recommended solution.

3. Issues to be solved in PV converters

In order to increase converter voltage pulse charging capacitors can work in parallel and be discharged in a serial circuit. To achieve high voltage gain it is necessary to charge and discharge them several times. This increases the number of components in the system. The advantage of this solution is the lack of magnetic components so the converter can be made in the form of a hybrid integrated circuit. An example of such solution is a switched capacitors converter integrated with a boost converter [2], which provides high voltage gain at a reasonable duty cycle and fairly high efficiency and adjustable output voltage. Another converter with switched capacitors is proposed in [3]. Basic principles of resonant energy transfer between switched capacitors and their impact on the number of degrees of voltage gain were explained in this article.

Another approach presented in [4] and [5] is to introduce a family of coupled-inductor converters. The use of a coupled-inductor converter can enable high voltage gain without the necessity to work at the highest duty cycle. However, the leakage inductance of a coupled-inductor may result in additional voltage overshoots across the switches which can increase switching losses and reduce the efficiency of the converter.

Application of a voltage clamp on the switch may reduce switching power losses and thus transistors with lower rated voltage can be used. In publications [4] and [5] a boost converter with a high voltage gain (up to 20) and high efficiency (up to 97%) was presented. In order to increase voltage gain the converter operation should be based on the use of a coupled-inductor with a series switched capacitor. Moreover, the clamp circuit recovers energy stored in leakage inductance ensuring high efficiency of this topology. In publication [6] a coupled-inductor boost converter with an output voltage doubler was presented. In this topology the output voltage is the sum of the classical boost converter voltage and twice amplified output voltage. The converter can operate at a duty cycle $D < 0.5$ and can be easily modified in order to obtain high voltage gain. Currently, there are many known converter topologies and it is not an easy task to choose the one with the best performance. Selection should be carried out taking into account the complexity of the converter. An estimation of the cost, size, weight, power level and the expected efficiency should be performed. During the practical implementation of the project the following questions should be answered:

- Can a non-isolated DC/DC converter operate with a high voltage gain $B > 10$ ($V_i = 20$–45 V, $V_o = 400$ V or ± 400 V) such as transformer isolated converters?
- How to increase the voltage gain B without necessity to work at extreme values of duty cycle $D < 0.7$, due to reduced input current ripples and capacitor sizes?
- Which non-isolated DC-DC converter topology is the best solution to use in PV systems?
- How to increase the efficiency of the PV inverter in the power range of 1 kW to 10 kW, to reach η near 0.98?
- How to reduce the voltage across the power transistor to reduce the costs of semiconductors and conduction losses?
- How to reduce the reverse recovery current of output diodes?
- Does the usage of SiC components bring tangible economical effects?

The problems to be solved for the next generation of non-isolated interfacing DC/DC converters are: increasing voltage gain and simultaneously obtaining low costs and high efficiency.

4. Isolated boost converters

In photovoltaic systems peak power is reached at a low level of input voltage, thus available system peak power is directly affected by the power losses in the converter. For this reason the power source must be oversized in order to compensate for the reduced efficiency of the converter. In addition, a thermal calculation of the power converter itself needs to be dimensioned for peak power dissipation which further increases the size and cost of the converter.

A large number of alternative converter topologies and implementations have been proposed typically achieving high conversion efficiency at the medium to high input voltage range and at medium power levels. Best in class designs achieve peak efficiencies up to 96%. Efficiency typically drops significantly to 90% or below at maximum output power and minimum input voltage.

Recent isolated boost converters achieve efficiencies of 97% to 98% with 30 to 50 V of input voltage and maximum output power of 10 kW [7, 8].

Buck converters are typically used in isolated converters systems. Contrary to popular belief, a properly designed boost topology is superior in performance to a buck topology and more appropriate for low voltage applications, as indicated by measured results [9].

In terms of average power a good choice is to use an isolated full-bridge boost converter with voltage doubler shown in Fig. 1 [9, 10]. Inverter bridge transistors S1 to S4 operate

in pairs S1 to S2 and S3 to S4. The drive signals are π radians phase shifted. Switch-transistor duty cycle is above 0.50 to ensure switch overlap time, and thus a continuous current path for the inductor L_1 current. Because of a very high input current primary switch conduction losses are a dominant loss factor in high-power low-voltage converters. Thus, optimum design and selection of primary switches are obviously very important in achieving high conversion efficiency. Total conduction losses in the primary switches of a full-bridge boost converter (number of switches $ns = 4$) is described in the following relationship:

$$P_{S,con,boost} = R_{on}\,(3 - 2D)\left(\frac{P_o}{\eta V_i}\right)^2, \qquad (1)$$

where P_o is the converter output power and η is efficiency of the converter ($\eta \approx 1$).

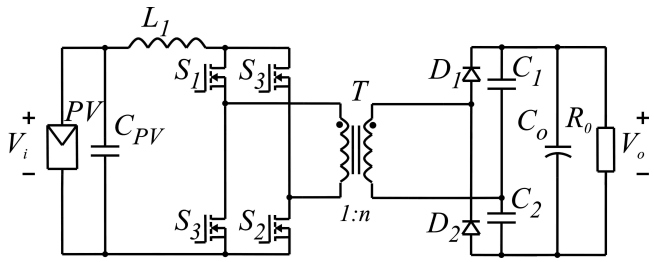

Fig. 1. An isolated full-bridge boost converter with voltage doubler

As it can be seen from Eq. (1) for a given output power, conduction losses decrease with increasing input voltage, but rise with increasing conduction resistance R_{on} of the transistor and the duty cycle.

During conduction, a diode voltage drop can be modelled by a fixed forward voltage drop V_D, in series with a resistive element R_D. Total rectifier conduction loss in an isolated boost converter with voltage doubler (two diodes) is equal to:

$$P_{D,con} = 2\left[\frac{P_o}{V_o}V_D + R_D\,(1 - D)\left(\frac{P_o}{nV_i}\right)^2\right], \qquad (2)$$

where $n = Ns/Np$ is the transformer turns ratio. Diode series resistance has the biggest impact on rectifier conduction losses because the product nV_i of the transformer turns ratio and input voltage can be regarded as a constant. Rectifier switching losses, in case of using SiC Schottky diodes, have a negligible share in the balance of total losses and therefore are negligible.

The voltage gain as a function of the duty cycle and transformer turns ratio is given by:

$$B = \frac{V_o}{V_i} = \frac{n}{1 - D}, \qquad (3)$$

where D is the switch duty cycle ($0.5 \leq D < 1$).

The peak efficiency reached 98%. In the worst case (the input voltage of 30 V) minimum efficiency of 96.8% was achieved in the range between 0.8 to 1.5 kW of output power, at the switching frequency $f_s = 45$ kHz. The duty cycle was $D = 0.7$, the transformer turns ratio was $n = 4$, conduction resistance equalled $R_{on} = 3.3$ mΩ, and input voltage was 50 V.

It should be noted that the inverter transistors and the rectifier diodes conduction losses are 28% and 29% respectively in the inverter power losses budget. The losses in the inductive elements comprise 24% of total losses [10, 11]. Test results from a 1.5 kW prototype converter confirmed the achievement of fast current switching, low parasitic circuit inductance and very high efficiency.

a)

b)

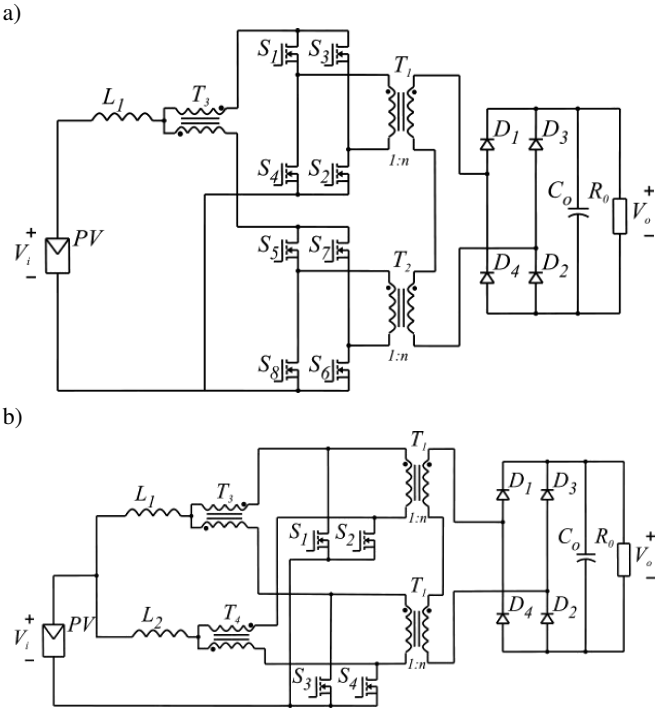

Fig. 2. Parallel isolated boost converters: a) primary-parallel isolated full-bridge boost converter, b) partially paralleled two-inductor-boost converter

The normalized voltage across the switches of the inverter

$$V_{DS,off} = \frac{V_o}{2n} = \frac{V_i}{2\,(1 - D)} \qquad (4)$$

depends on input voltage and duty cycle, but is not dependent on output power and ranges from 50 V to 83 V for input voltages from 30 V to 50 V and $D = 0.7$.

A simple and low cost method of extending the power level in isolated boost converters is to parallel the critical high-ac-current parts of the circuit (Fig. 2). The partial parallel isolated boost converter is depicted in Fig. 2a [8]. Two primary side inverter bridges consisting of S1 to S4 and S5 to S8 respectively operate in-synchronism and in-phase, utilizing the same control signals. Each inverter bridge supplies a power transformer. Small volt-time product imbalances between the two power stages which are caused by small differences in gate driver delays, power MOSFET switching speed, and/or parasitic circuit elements, are absorbed by the current balancing transformer.

Within the power range of 2 to 3 kW output and an input voltage of 50 V, peak efficiency reached 98%. In the worst

case when the input voltage was 30 V, the minimum efficiency reached 96.9% at maximum output power. The inverter transistors conduction losses (28%) and the rectifier diodes (29%) did not change. The losses in the inductive components constitute 18% of total losses. The total turn-off loss was shared between all switches and corresponds to only 0.7% in efficiency decrease. It should be noted that switching losses are very low and that conduction losses constitute more than 70% of all losses [8].

The partial paralleling method can also be applied to all other isolated boost converters. As an example the implementation of a partially paralleled two-inductor-boost converter [10] is presented in Fig. 2b. Extension to a higher number of paralleled converter stages is possible through adding an extra current balancing transformer for each extra parallel power stage. For even numbers of paralleled power stages the current transformer turns ratio should be 1:1. For odd numbers of paralleled power stages, one current transformer needs to have a turns ratio of 2:1. Extra odd numbered power stage should be equipped with a winding having a higher number of turns. In general, $N-1$ current balancing transformers are needed for paralleling N power stages. Appropriate design of power transformers which will have very low leakage inductance is crucial to obtain very high efficiency.

Previously it was believed that high transformer turns ratio, required in high gain applications causes large transformer leakage inductance. However, as explained in [7], the real problem in high frequency power transformers with high current windings is the elimination of high winding AC-resistance because of the strong impact of proximity effect.

Transformer windings can be grouped into a number of winding portions and intersections according to their magnetomotive force. Winding intersections create small volumes of constantly high magnetic field strength. In winding portions the magnetic field strength increases linearly from zero to maximum.

In multi layer windings the increase in winding AC resistance R_{ac}, relative to winding DC-resistance R_{dc} with sinusoidal excitation at a specific frequency caused by the eddy current effect, is equal to

$$F_R = \frac{R_{ac}}{R_{dc}} = \varphi \frac{\sinh 2\varphi + \sin 2\varphi}{\cosh 2\varphi - \cos 2\varphi} + \\ + \frac{2\left(m^2-1\right)}{3} \varphi \frac{\sinh \varphi - \sin \varphi}{\cosh \varphi + \cos \varphi}, \tag{5}$$

where $\varphi = h\delta$, and h is the height of the conductor, δ is the penetration depth into the material, and m is the number of layers in a winding portion.

The transformer winding resistance factor in a quadruple interleaved converter ($M = 4$) becomes 7.7 times smaller then in one without an interleaving transformer ($M = 1$).

An analysis of transformer leakage inductance, in the work of Andersen and Nymand [11], shows that transformer leakage inductance does not depend on transformer turns ratio. Extensive interleaving of primary and secondary windings is needed to reduce the proximity effect which significantly reduces transformer leakage power losses.

Transformer leakage inductance with intersections is given by:

$$L_l = \mu_0 \frac{l_w h_w N^2}{3 b_w M^2}, \tag{6}$$

where μ_0 is the permeability of free space, l_w is the mean turn length, h_w is the total height of transformer winding, b_w is the breadth of winding, N is the number of winding turns, and M is the number of primary-secondary intersections.

Using (6), the leakage inductances for the two winding configurations were calculated. The leakage inductance in the conventional winding configuration (M=1) is approximately 35 times greater than corresponding leakage inductance in the octuple interleaving configuration ($M = 8$).

Above considerations show that extensive interleaving of primary and secondary windings will lead to very little energy stored in transformer leakage inductance. The leakage inductance is proportional to the number of turns squared N^2. The small number of turns required on primary windings of low-voltage high-power transformers will cause extremely small leakage inductance. Transformer leakage inductance for a given winding does not depend on the number of turns of other windings.

For this reason the leakage inductance in a transformer is not a function of transformer turns ratio but depends only on the winding manufacturing technique and the number of turns on the specific winding.

Low complexity, low cost and very high conversion efficiency makes the proposed converter an optimum choice for high-power high-gain converter applications.

Further calculations are carried out with the same parameters, including appropriate conduction resistance value of R_{on} which is related to the maximum value of voltage blocking switches.

5. Non-isolated interleaved coupled-inductor boost converters

The non-isolated coupled-inductor boost converter (Fig. 3a) can be a good solution to issues occurring with the conventional boost converter discussed above. This is because coupled inductor windings cause an increase in output voltage. That can be effectively used to reduce the duty cycle and the voltage stress of the switch. Therefore, for high-voltage step-up applications, the coupled inductor boost converter can be more efficient than the conventional boost converter [12–16] and single phase full bridge inverter with coupled filter inductors and voltage doubler [17].

The voltage gain of the coupled-inductor boost converter can be obtained by:

$$B = \frac{1 + nD}{1 - D}. \tag{7}$$

With an ideal coupling between the primary and secondary windings the voltage across the transistor

$$V_{DS,off} = \frac{nV_i + V_o}{n+1} = \frac{V_i}{1-D} \tag{8}$$

does not depend on the parameters of the inductor. It is always higher than the input voltage and at high duty cycle can reach significant values. Moreover, the voltage overshoots caused by parasitic parameters are present in practical circuits. It induces additional voltage stresses and necessitates the use of switches with higher blocking voltage, leading to more losses. Handling of very large input currents from low-input voltage sources remains a practical issue for high power applications.

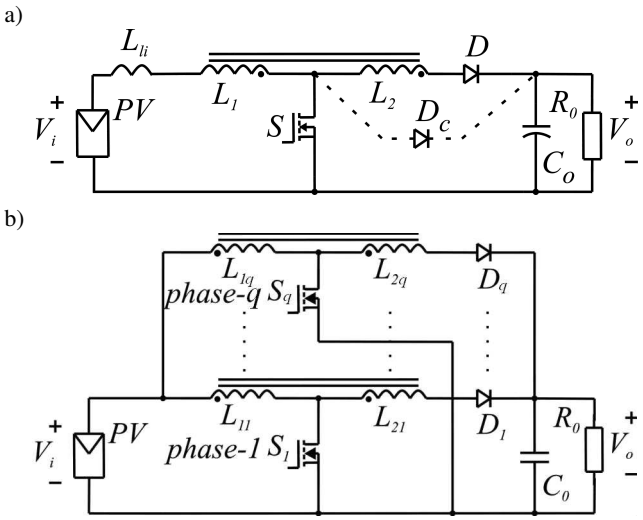

Fig. 3. Non-isolated coupled-inductor boost converters a) coupled-inductor boost converter, b) interleaved coupled-inductor boost converter

Due to the less than ideal coupling between the primary and the secondary windings of the coupled inductors, leakage inductances occur. These cause high-voltage spikes across the switch and as a result additional losses are introduced when the switch is turned off. Voltage overshoots can be reduced by applying a parallel diode D_c (Fig. 3a), through which the energy stored in the leakage inductance is transferred to the output. Switch voltage is clamped to the output voltage. Due to the high output voltage it is necessary to use high-voltage transistors with relatively high turn-on resistance R_{on}. Unfortunately high resistance causes an increase in conduction losses and reduces the efficiency of the converter.

The number of parallel phases q in an interleaved converter (Fig. 3b) mainly depends on the maximum power demand of the load and the maximum power rating of the interleaved phases. All the phases operate at the same duty cycle but they are phase shifted by $2\pi/q$ radian electrical angle. Due to interleaving the switching frequency is q times higher than the switching frequency of a single phase. Under lower output power demand the number of operating phases can be adjusted for maximally efficient operation of individual phases.

Various converters which utilize magnetically coupled inductors, which reduce the extreme duty cycle operation for non-isolated high step-up applications, are reported in literature [18] to [21]. These, however, are not suitable for high current and high power applications, and moreover, the circuits are complex to design and model.

To process high power and to achieve high efficiency as well as high reliability with reduced size of inductors and capacitors, interleaving coupled-inductor boost converters are recommended for high-input current applications [21].

The coupled-inductor boost converter and interleaved coupled-inductor boost converter with single boost converter clamp (Fig. 4) can be good solutions to the problems discussed above [22]. Coupled inductors reduce the required duty cycle for a given voltage gain. This also reduces the voltage across the switch. The duty cycle and the switch voltage stress can be controlled by the turns ratio of the primary inductor $L1$ to secondary inductor $L2$. The number of parallel phases in an interleaved converter mainly depends on the maximum power demand of the load and the maximum power rating of the interleaved phases. An efficient high power converter with a reduced size output filter can be obtained through an interleaving technique.

To lower voltage stress on the switches to the level of the voltage stress present in an ideal coupled-inductor boost converter, a common active-clamp circuit based on a boost converter can be used (Fig. 4) [22].

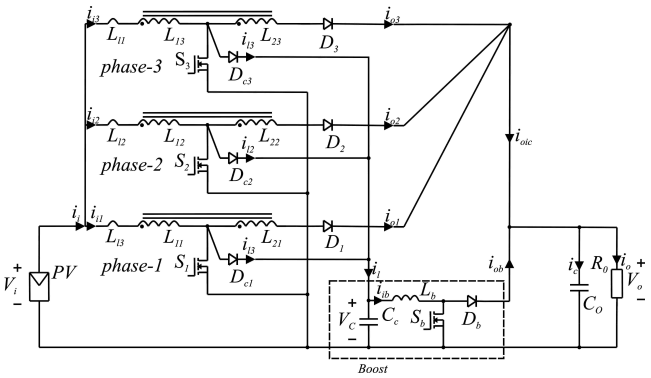

Fig. 4. Interleaved coupled-inductor boost converter with single boost converter clamp (for $q = 3$)

Energy stored in the leakage inductors of the interleaved phases is discharged through the clamp diodes D_c and gathered in the clamp capacitor C_c. A boost converter is used to transfer the stored energy in the clamp capacitor to the output of the converters, while maintaining the voltage level of the clamp capacitor at a lower level (Fig. 4).

The voltage rating of the switches S_1, S_2 and S_3 of the coupled-inductor boost converters is determined by the value of the clamp voltage and can be expressed as:

$$V_c \approx V_{DS,off} = V_i \left(1 + \frac{DK}{1-D}\right), \tag{9}$$

where $K = \frac{L_{\mu 1}}{L_{\mu 1}+L_{l1}}$, $L_{\mu 1}$, L_{l1} are magnetizing inductance and leakage inductance of the primary winding coupled-inductor respectively.

The steady state voltage gain for an ideal converter can be obtained by:

$$B = 1 + \frac{(1+n)\,D}{1-D}K. \tag{10}$$

For input voltages from 30 V to 50 V, $D = 0.7$, $K = 0.97$ voltages across transistor can be as much as 98 V to 163 V respectively.

In order to compare a non-isolated converter (Fig. 2) with an isolated converter (Fig. 4), formulas (7) and (8) are used to formulate the following expression:

$$q = \frac{V_o\left[1 - D\left(1 - K\right)\right] - V_c}{DKV_c}. \tag{11}$$

Assuming the same voltage across the transistor and the output voltage, the same as in an isolated converter (V_c = 50 V, V_o = 400 V), the number of phase $q = 10$ can be obtained for the duty cycle $D = 0.7$, which will ensure the same across transistor voltages. However from a practical point of view parallel connection of the ten basic converters is not feasible.

The measured efficiency was equal to 94.8%. at following conditions: output power of 1.5 kW, input voltage of 42 V, output voltage of 350 V, and switching frequency of 25 kHz.

Losses in MOSFET transistors, diodes and inductive elements of interleaved coupled-inductor converter were 29%, 11% and 36% respectively, with the boost converter constituting 7% of the total converter power losses [22].

6. Non-isolated boost converters based on three-state switching cell

A non-isolated push-pull-boost converter is presented in Fig. 5. Diodes D1, D11 and a capacitor C1 – act as a regenerative snubber, recycling energy stored in a leakage inductance of the push-pull transformer. Series connection of all capacitors improves voltage gain. In literature this topology is also called a boost converter with a three state switching cell and a voltage multiplier [23]. The converter operates in continuous current mode and with duty cycle above 50%.

The voltage gain is described by the following equation:

$$B = \frac{1 + nk}{1 - D} = \frac{1 + n}{1 - D}, \tag{12}$$

where k is the number of secondary winding ($k = 1$), and n is the transformer turns ratio.

The maximum voltage across active switches S1 and S2, without considering voltage overshoots due to layout inductances and the maximum reverse voltages across both diodes D1 and D11, are given as:

$$V_{DS,off} = V_{D,R} = \frac{1}{1 + n}V_o = \frac{V_i}{1 - D}. \tag{13}$$

The maximum reverse voltages across diodes D2 and D3 are $n$times higher than the voltages specified in the Eq. (11). The maximum possible turns ratio value should be chosen for a particular design. The higher it is the lower is the voltage stress across the switches and diodes D1 and D11 calculated by (11).

For input voltages of 30 V to 50 V at $D = 0.7$ voltage transistors and diodes are within 100 V to 167 V respectively.

Comparing equations (4), (7) and (11), which determine the maximum voltage across transistors, it is concluded that in the isolated converters voltages are twice lower than in a non-isolated push-pull-boost converter.

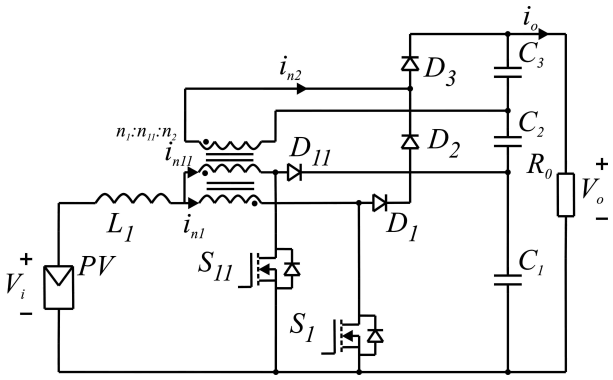

Fig. 5. Non-isolated push-pull-boost converter (n=n_2/n_1=n_2/n_{11})

Total conduction losses in the primary switches of a non-isolated push-pull-boost converter are given by

$$P_{S,con,boost} = R_{on}\frac{1-D}{2}\left[\left(\frac{2n+1}{n+1}\right)^2 + \frac{2D-1}{1-D}\right]\left(\frac{P_o}{V_i}\right)^2. \tag{14}$$

Total conduction losses in MOSFETs were calculated using equations (1) and (12). Losses in the primary-parallel isolated full-bridge boost converter (R_{on} = 3.3 mΩ, $n = 4$) are about 30% higher than losses in the non-isolated push-pull-boost converter (R_{on} = 13 mΩ, $n = 2$).

The major advantages of this topology are: a limited input current ripple, the input inductor operates with twice the switching frequency allowing weight and volume reduction, and the voltage stress across the transistors is lower than half the output voltage. It is also important to notice that for a given duty cycle, the output voltage can be increased by incrementing the transformer turns ratio without exposing the transistors to voltage stress. Disadvantages of the converter are: three series connected output capacitors and the number of diodes connected in series. The converter does not operate appropriately for a duty cycle lower than 0.5 due to magnetic induction problems of the transformer.

However, in spite of these drawbacks this topology seems to be a good solution for a boost converter in photovoltaic systems.

In studies of non-isolated push-pull-boost converter with power of 500 W and at 45 V of input voltage, an efficiency of 97.5% was achieved. In the worst case for maximum output power, with the input voltage at 30 V, efficiency decreased to 97% [24]. For a converter with a power of 1 kW and input voltages of 30V peak efficiency was equal to 96.8% at 400 W, and for maximum output power was equal to 95.5% [25].

In order to reduce leakage inductance and proximity effect between the layers an autotransformer interleaved winding was applied.

Non-isolated two-inductor-boost converter shown in Fig. 6 has similar properties [25]. The voltage gain of this topology

$$B = \frac{1 + 2n}{1 - D} \tag{15}$$

is $(1+2n)/(1+n)$ times higher in comparison with the non-isolated push-pull-boost topology.

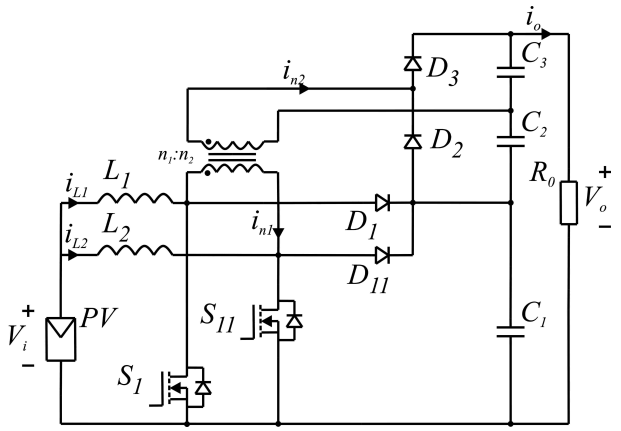

Fig. 6. Non-isolated two-inductor-boost converter ($n = n_2/n_1$)

The voltage across switches S1 and S2 and reverse voltages across the diodes D1 and D11 are given by

$$V_{DS,off} = V_{D,R} = \frac{1}{1+2n} V_o. \tag{16}$$

The maximum reverse voltages across diodes D2 and D3 are n times higher than the voltages specified in the Eq. (16).

Total conduction losses in the primary switches of a non-isolated two-inductor-boost converter are given by

$$P_{S,con,boost} = R_{on} \cdot \left[(1-D) \left(\frac{1}{2} + \frac{n}{1+2n} \right)^2 + \frac{2D-1}{4} \right] \left(\frac{P_o}{V_i} \right)^2 \tag{17}$$

and they are 2.5 times lower than in the push-pull-boost converter.

This topology has similar features to a non-isolated push-pull boost converter. It includes a high voltage gain, reduced voltage stress on transistors and smooth input current. This topology utilizes a simple two-winding transformer instead of a more complex three-winding one. Main drawbacks of this topology are several diodes connected in series and three series connected output capacitors.

Non-isolated push-pull-boost and a non-isolated two inductor-boost topologies are more complex then a basic boost converter and they require more components, but they provide better utilization of switches requiring a smaller number of passive components. Also, these two topologies have higher voltage gains so they operate at a lower duty cycle than the basic boost converter.

Despite the drawbacks mentioned these topologies are a good solution for photovoltaic systems.

7. Conclusions

Discussed selection of the boost DC/DC converters to interface low-voltage high-power supply to the mains indicates that the highest efficiency (over 98%) was achieved in the primary-parallel isolated full-bridge boost converter. Non-isolated converters, interleaved coupled-inductor boost converters with single boost converter clamp and boost converters may have slightly lower efficiency, but they gain in size, since the number of passive components is reduced. They also provide a better utilization of switches, have better voltage gain and are able to work at a lower duty cycle in comparison to other non-isolated boost converters.

Boost converters are usually equipped with overvoltage protection circuits. In some selected isolated topologies the overvoltage protection circuits are useless since inductive components and circuit configuration are optimized to work under low input voltage and high power. In other converter topologies the energy stored in the leakage inductance of inductive components is transferred to the output capacitors and that eliminates voltage overshoots across power switches. An analysis of transformer leakage inductance shows that not only does it not depend on transformer turns ratio, but that the extensive interleaving of primary and secondary windings needed to reduce the proximity effect, significantly reduce transformer leakage energy. High power and low input voltage cause the converter input impedance to be very low. That requires low values for effective R_{AC} resistance and parasitic inductance dissipation to achieve high efficiency of energy conversion.

High input current requires large area of cross-sectional winding inductors. To avoid the serious consequences of the proximity effect a minimum possible number of layers of windings must be properly positioned and interleaved in sections. In both isolated and non-isolated boost converters very small leakage inductance and very low energy in the inductive components can be achieved, contrary to generally accepted views, through proper design of magnetic components. Oversizing the rated voltage of power switches leads to a sharp increase of conduction losses. Highest efficiency can be achieved by using switches with lower values of blocking voltages.

Power switches in interleaved converters, compared to the switches used in non-interleaved ones, work at lower values of effective currents. This allows the use of switches with better static and dynamic parameters during parallel work. The main goal of interleaved converters is to provide the same cycle for all transistors. Even a slight difference in cycles may lead to imbalance and reduce system reliability.

In spite of the cost higher than that of conventional converters of interleaved power converters, the potential gain of efficiency will bring tangible economic effects throughout the lifetime of the converter. The use of boost modular converters can improve the efficiency of PV systems. When designing modular converters the output power theoretically is not limited. Efficiency can be increased by turning-off one or more modules, depending on light intensity.

Application of SiC Schottky diodes in output circuits eliminates the reverse recovery problems, and thus allows quick diode turn-off without significant power losses. Figure of merit indicates a large potential in application of SiC devices in low-voltage high-power boost converters. Commercially available SiC high-voltage semiconductor devices allow significant reduction of losses in comparison to the components of Si

with similar blocking voltage. Still there are no SiC transistors available on the market, which have a lower conduction resistance than the Si MOSFET counterparts.

Acknowledgements. The project was financed by the National Science Center under the project No. N N510 512040.

REFERENCES

[1] T Kerekes, R. Teodorescu, P. Rodríguez, G. Vázquez, and E. Aldabas, "A new high-efficiency single-phase transformerless PV inverter topology", *IEEE Trans. on Indust. Electronics* 58 (1), 184–191 (2011).

[2] O. Abutbul, A. Gherlitz, Y. Berkovich, and A. Ioinovici, "Step-up switchingmode converter with high voltage gain using a switched-capacitor circuit", *Circuits and Systems I: Fundamental Theory and Applications, IEEE Trans. on Circuits and Systems* 50, 1098–1102 (2003).

[3] K.K. Law, K.W.E. Cheng, and Y.P.B. Yeung, "Design and analysis of switched-capacitor-based step-up resonant converters", *Circuits and Systems I: Regular Papers, IEEE Trans. on Circuit Systems* 52, 943–948 (2005).

[4] W. Rong-Jong and D. Rou-Yong, "High step-up converter with coupled inductor", *Power Electronics, IEEE Trans. on Power Electronics* 20, 1025–1035 (2005).

[5] R.J. Wai and R.Y. Duan, "High-efficiency DC/DC converter with high voltage gain", *Electric Power Applications, IEE Proc.* 152, 793–802 (2005).

[6] B. Ju-Won, R. Myung-Hyo, K. Tae-Jin, Y. Dong-Wook, and K. Jong-Soo, "High boost converter using voltage multiplier", *Indust. Electronics Society, 31st Annual Conf. IEEE* 1, 567–572 (2005).

[7] M. Nymand, R. Tranberg, M.E. Madsen, U.K. Madawala, and M.A.E. Andersen, "What is the best converter for low voltage fuel cell applications- a buck or boost?", *Proc. IEEE IECON* 1, 959–964 (2009).

[8] M. Nymand and M.A.E. Andersen, "High-efficiency isolated boost dc-dc converter for high-power low-voltage fuel cell applications", *IEEE Trans. Indust. Electronics* 57 (2), 505–514 (2010).

[9] M. Nymand and M.A.E. Andersen, "A new approach to high efficiency in isolated boost converters for high-power low-voltage fuel cell applications", *Proc. EPE-PEMC* 1, 127–131 (2008).

[10] M. Nymand and M.A.E. Andersen, "New primary-parallel boost converter for high-power high gain applications", *Proc. APEC* 1, 35–39 (2009).

[11] M. Nymand, U.K. Madawala, M.A.E. Andersen, B. Carsten, and O.S. Seiersen, "Reducing ac winding losses in high-current high-power inductors", *Proc. IEEE IECON* 1, 774–778 (2009).

[12] W. Li. and X. He, "An interleaved winding-coupled boost converter with passive lossless clamp circuits", *IEEE Trans. on Power Electronics* 22 (4), 1499–1507 (2007).

[13] W. Li. and X. He, "A family of interleaved DC–DC converters deduced from a basic cell with winding-cross-coupled inductors (WCCIs) for high step-up or step-down conversions", *IEEE Trans. on Power Electronics* 23 (4), 1791–1801 (2008).

[14] K. Hirachi, M. Yamanaka, K. Kajiyama, and S. Isokane, "Circuit configuration of bidirectional DC/DC converter specific for small scale loading system", *Proc. PCC-Osaka* 2, 603–609 (2002).

[15] S. Dwari, S. Jayawant, T. Beechner, S.K. Miller, A. Mathew, M. Chen, J. Riehl, and J. Sun, "Dynamics characterization of coupled-inductor boost DC-DC converters", *Proc. Computers in Power Electronics, IEEE Workshop* 1, 264–269 (2006).

[16] S. Pirog , R. Stala, and L. Stawiarski, "Power electronic converter for photovoltaic systems with the use of FPGA-based real-time modeling of single phase grid-connected systems", *Bull. Pol. Ac.: Tech.* 57 (4), 345–354 (2009).

[17] Y. Jiang and J. Pan, "Single phase full bridge inverter with coupled filter inductors and voltage doubler for PV module integrated converter system", *Bull. Pol. Ac.: Tech.* 57 (4), 355–361 (2009).

[18] C.M.C. Duarte, and I. Barbi, "An improved family of ZVS-PWM active clamping DC-to-DC converters", *IEEE Trans. Power Electronics* 17 (1), 1–7 (2002).

[19] W. Rong-Jong, and D. Rou-Yong, "High step-up converter with coupledinductor", *IEEE Trans. on Power Electronics* 20 (5), 1025–1035 (2005).

[20] W. Rong-Jong, and D. Rou-Yong, "High-efficiency power conversion for low power fuel cell generation system", *IEEE Trans. Power Electronics* 20 (4), 847–856 (2005).

[21] S. Dwari and L. Parsa, "A novel high efficiency high power interleaved coupled-inductor boost DC-DC converter for hybrid and fuel cell electric vehicle", *Proc. IEEE Vehicle Power Propulsion Conf.* 1, 399–404 (2007).

[22] S. Dwari and L. Parsa, "An efficient high-step-up interleaved DC–DC converter with a common active clamp", *IEEE Trans. on Power Electronics* 26 (1), 66–78 (2011).

[23] P. Zacharias, B. Sahan, S.V. Araújo, F.L.M. Antunes, and R.T. Bascopé, "Analysis and proposition of a PV module integrated converter with high voltage gain capability in a non-isolated topology", 7th *Int. IEEE Conf. on Power Electronics* 1, CD-ROM (2007).

[24] P. Klimczak and S. Munk-Nielsen, "High efficiency boost converter with three state switching cell", *Int. Exhibition & Conf. Power Electronics, Intelligent Motion, Power Quality PCIM* 1, 143–148 (2009).

[25] P. Klimczak, "Modular power electronic converters in the power range 1 to 10 kW", *PhD Thesis*, Aalborg University, Denmark Institute of Energy Technology, Aalborg, 2009.